Influence of the Structural Changes During Alkaline Cooking on the Thermal, Rheological, and Dielectric Properties of Corn Tortillas

M. E. RODRÍGUEZ,[1] M. YÁÑEZ-LIMÓN,[1] J. J. ALVARADO-GIL,[1] H. VARGAS,[1,2] F. SÁNCHEZ-SINENCIO,[1] J. D. C. FIGUEROA,[3] F. MARTÍNEZ-BUSTOS,[3] J. L. MARTÍNEZ-MONTES,[3] J. GONZÁLEZ-HERNÁNDEZ,[3] M. D. SILVA,[4] and L. C. M. MIRANDA[4]

ABSTRACT

Cereal Chem. 73(5):593–600

Basic data on thermal, dielectric, and infrared spectra properties of cooked tortillas were investigated with the aim of understanding the role of lime, Ca(OH)$_2$, that is incorporated during the alkaline cooking process. The data are further supplemented by X-ray diffraction and texture measurements. The changes in the thermal diffusivities, as measured by the photoacoustic technique, as well as changes in texture, X-ray patterns, dielectric, and infrared spectra properties are presented as a function of the lime concentration. The results show strong evidence that there is a marked concentration of lime at ≈0.2% above and below where there are different behavior patterns of the measured properties of tortilla. In particular, the results of the study of dielectric constants and thermal diffusivity provide strong evidence for an enhancement of the starch crosslinking taking place at a lime content of ≈0.2 %.

In the last decade, the physical properties of food solids have received increasing attention (Simatos and Karel 1988, Slade et al 1989, Roos and Karel 1991) not only because of their importance to food processing and shelf life, but also due to the scientific interest in the challenging structural and molecular transitions that take place in these biopolymers (Hollinger et al 1974, Donovan 1979). In general, food and biological solids are in an amorphous metastable state that is very sensitive to changes in temperature and moisture content such as those occurring in natural storage or in cooking. Usually, the amorphous state results from rapid removal of water by drying or freezing (Levine and Slade 1988, Alexander and King 1985). The amorphous matrix may exist either as a very viscous glass or as a more liquid-like "rubbery" amorphous structure. The change from the glassy to the rubbery state occurs at a glass transition temperature specific to each material. Like water however, plasticizers can decrease the glass transition temperature. The influence of the glass transitions of dried and frozen foods on the chemical and physical changes during food processing and storage have been reported by several authors (Herrington and Brandfield 1984, Roos 1987). Above the glass transition temperature, molecular mobility is greatly increased and many amorphous compounds crystallize. This crystallization may take place as either temperature or moisture content is increased. For instance, amorphous lactose was reported to crystallize rapidly at room temperature and ≈40% relative humidity (Saltmarch and Labuza 1980).

Among the various biopolymers the food industry deals with, starch is undoubtedly one of the most important. As compared to natural cellulosic systems, starch is readily accessible, and modifications to rheological properties can be achieved through simple crosslinking reaction conditions. Furthermore, apart from its wide use in the chemical industry at large (adhesives, edible films, viscosity controller in oil drilling, paper thickener, etc.), baked starch plays a major role in our daily diet. In some Latin American countries, the main source of starch intake is through alkaline-cooked corn products (nixtamalized products) such as the Mexican tortilla. Tortillas alone provide 70% of the calories and half of the protein to the diet of some population in these countries. In the United States, alkaline cooking is used in the production of Mexican corn-based food products such as table tortillas, corn chips, and taco shells.

The importance of lime, Ca(OH)$_2$, in the alkaline cooking of corn has been investigated by several authors (Paredes-Lopez and Saharoupulos 1982, Trejo-Gonzalez et al 1982, Robles et al 1986, Gomez et al 1992). Still, the role the calcium plays in this process is not entirely understood. However, some important aspects of alkaline cooking are well known, and it is worthwhile mentioning them here. Alkaline cooking and steeping of corn causes water and calcium to be taken up by the grains. The alkaline solution degrades and solubilizes the cell wall components, resulting in the removal of pericarp and softening of the endosperm structure. A small amount of amylose leaching occurs after the starch granules swell, which contributes to the formation of a network of cellular components. At pH values of 11 and higher, the amylose molecules carry negative charge, allowing interaction with the calcium ions (Trejo-Gonzalez et al 1982). According to Robles et al (1986), the gelatinization of starch during alkaline cooking and steeping of corn is inhibited by the amylose-calcium interaction. Amylose retrogradation occurring during corn steeping results in the recovery of the native starch crystallinity (Gomez et al 1992).

Most of the studies on corn alkaline cooking have focused on the changes in structural and rheological properties obtained from X-ray diffraction, viscosity, and microscopic analysis. In a recent article (Alvarado-Gil et al 1994), we reported on the photoacoustic monitoring of tortilla processing conditions. In this article, we report on the monitoring of the changes in the dielectric, thermal, and infrared spectra properties of cooked tortillas as a function of lime content. These data are further supplemented by crystallinity and texture measurements aimed at understanding the changes induced by lime content on these physical properties. In particular, thermal diffusivity was studied using photoacoustic spectroscopy (Vargas and Miranda 1988).

MATERIALS AND METHODS

Whole corn meal, water (65%, w/w, final concentration), and different amounts of calcium hydroxide were mixed and used as starting materials. The mixture was processed in a low-shear

[1]Departamento de Física, Centro de Investigación y de Estudios Avanzados del IPN, AP 14-740, México, D.F. 07000.
[2]Corresponding author. E-mail: fisjja@fis.cinvestav.mx
[3]Laboratorio de Investigación en Materiales, Universidad Autonoma de Querétaro, Facultad de Química, Centro Universitario C. de las Campanas, Querétaro, Qro México 76010.
[4]Laboratório de Sensores e Materiais, Instituto Nacional de Pesquisas Espaciais, 12227-010, Sao José dos Campos, S.P., Brazil.

extruder with a barrel temperature of 65°C and a screw speed of 35 rpm to produce fresh masa with the appropriate characteristics for dehydration and milling to obtain instant dry masa flour. Instant dry masa flour was rehydrated with 70% water to obtain fresh masa at the appropriate consistency to make tortillas. Tortillas were made from 30 g of fresh masa shaped into discs that were ≈10 cm in diameter and 0.2 cm thick. The masa discs were baked on a hot plate at ≈290°C for 30 sec on one side, followed by baking for 40 sec on the opposite side, then the discs were turned again until puffing occurred. The cooking time was defined as the total time needed to observe puffing. The measured cooking time as a function of calcium hydroxide concentration is shown in Table I. The thermal diffusivity was measured in small pieces of tortilla (≈300 μm thick) that were rubbed with sandpaper to obtain samples with a smooth and flat surface. The samples used for the diffusivity measurements were previously dried overnight.

X-Ray Diffraction Analysis

The X-ray powder diffraction was also performed in dried samples. Tortillas were ground to a fine powder to pass through a screen with 150-μm openings. The samples in powder form were densely packed in an Al frame. X-ray diffraction patterns of samples were recorded on a Siemens D500 diffractometer operating at 35 kV, 15 mA with Cu Kα radiation wavelength λ = 1.5406 Å. Diffractograms were obtained from 4–30° on a 2θ scale with a step size of 0.05°. Data are reported as interplanar d-spacing values expressed in Å. The crystallinity (%) was calculated by normalizing the integrated diffracted intensity over the measured 2θ range to the integrated noncoherent intensity. The noncoherent intensity was obtained by subtracting the sharp diffraction peaks from the total diffraction pattern using the software Diffrac/AT from Socobin VI.2. Measurements in each sample were performed in duplicate. The numerical values of crystallinity (%) are shown in Table I.

Texture Analysis

Tortilla samples roughly 0.3 cm thick and ≈3.7 cm in diameter were used for the texture analysis. The tortillas firmness or texture as a function of $Ca(OH)_2$ concentration was measured using the Universal Texture Analyzer (Texture Technologies Corp., Scarsdale, NY) equipped with a TA-54 spherical-ended probe 4 mm in diameter. The head speed was run at 2 mm/sec. Firmness (breaking force) of tortillas is defined as the force (in kgf) required to stretch and finally break out the tortilla. The values reported for texture shown in Table I are the average values obtained from three independent measurements at room temperature.

Infrared Spectroscopy

The infrared transmission spectra between 400 and 4,000 cm⁻¹ were obtained using a 750 Magna-IR Nicolet spectrometer. Tortilla samples with different lime contents were ground to pass through a 50-μm mesh. The resulting powder was molded in the shape of discs 0.4 cm in diameter and ≈35 μm thick, to get samples with appropriate dimensions for the measurements. In these measurements, care was taken to subtract the background in each experimental run, after draining the system with dry air. In Table II, we summarize the results for the absorption coefficient for some selected infrared (IR) absorption bands as obtained from the IR transmission spectra using Beer's law.

Dielectric Properties Measurements

The dielectric measurements were made using a Schlumberger model SI1260 Impedance/Gain-Phase Analyzer operating at 200 preprogrammed frequencies between 1 Hz and 1 MHz, with a voltage amplitude of 3V. The samples used in the measurements were discs 0.25 cm thick and ≈12 cm in diameter. The errors in the dielectric constant values were <0.1% for frequencies above 100 kHz and ≈1% for frequencies below 10 kHz. Table III shows the measured values of the dielectric permitivity and ac conductivity as a function of lime concentration recorded at 10.2 kHz.

Thermal Diffusivity Measurements

The thermal diffusivity α can be accurately measured by the photoacoustic (PA) technique (Vargas and Miranda 1988). The PA measurements of the thermal diffusivity of polymers have been reported by a number of authors (Merté et al 1983, Lachaine and Poulet 1984, Torres-Filho et al 1989, Leite et al 1990). These studies employed different versions of the PA technique. Of the several PA techniques available for measuring thermal diffusivity, we used the "open cell" method (Perondi and Miranda 1987, Vargas and Miranda 1988, Mansanares et al 1990, Marquezini et al 1991). It consists of mounting the sample directly onto a cylindrical electric microphone and using the front air chamber of the microphone itself in place of the usual gas chamber in conventional photoacoustics. For the present case, samples are thermally thick, i.e., sample thickness is greater than the thermal diffusion length, $\mu = (\alpha/\pi f)^{1/2}$, where f is the modulation frequency of the incident light. Thermal diffusivity α is obtained from the PA signal data fitting from the coefficient $a = (\pi l^2/\alpha)^{1/2}$ in the expression for the amplitude for the PA signal:

$$S = (A/f) \exp(-a\sqrt{f}) \qquad (1)$$

The constant A in the measured signal S, apart from geometric parameters, includes factors such as the gas thermal properties, light beam intensity, and room temperature. The PA thermal diffusivity measuring set up shown in Figure 1 consisted of a 250W halogen lamp with a polychromatic beam modulated using a variable speed chopper (SR model 540) and later focused onto the sample. The microphone output voltage was measured using a lock-in amplifier (SR model 850). To make sure that the incoming light beam was absorbed at the front sample surface, thereby gen-

TABLE I
Effects of Lime Concentration on Thermal, Structural, and Rheological Properties of Cooked Tortillas

Physical Parameter	Lime Content (%)					
	0.0	0.1	0.2	0.25	0.3	0.5
Thermal diffusivity[a]	2.75	2.94	3.31	2.77	1.67	1.27
Cooking time (sec)	83	76	74	73	75	74
Crystallinity (%)	9.62	10.78	10.99	10.66	9.90	9.66
Firmness (kgf)	7.93	5.73	4.10	4.0	3.17	7.19

[a] ($\times 10^{-2}$ cm²/sec) ±0.3%.

TABLE II
Values of the Fitted Parameters[a] for the Infrared Absortion Coefficients

Absortion Bands (cm)	β_0	$\Delta\beta$	χ_c	$\Delta\chi$
2,925	159.25	38.38	0.1899	0.0042
3,350	156.63	27.37	0.1765	0.0061
1,458	111.09	18.83	0.1682	0.0066
710	118.50	27.82	0.1639	0.0136

[a] χ = crystallinity β = absorption coefficient.

TABLE III
Dielectric Permitivity and Conductivity Recorded at 10.2 kHz

Lime Content (%)	Dielectric Constant	Conductivity[a]
0.0	35.95	2.43
0.10	30.38	1.96
0.15	65.01	5.51
0.20	74.03	6.21
0.25	55.55	4.54
0.30	62.29	4.71
0.50	58.15	4.24

[a] $(\Omega \text{ cm})^{-1} \times 10^7$

erating a surface heating of the sample, we attached a thin circular Al foil (20 μm thick and 0.5 cm in diameter) to the front of the sample using a thin layer of vacuum grease.

The thermal diffusion time in this Al foil is on the order of 13.6 μsec, so that the heat generated in the Al absorber may be assumed to be instantaneously transmitted to the sample. In Figure 2, we show the PA signal amplitude as a function of the frequency square root for a tortilla 300 μm thick without lime. The solid curve in this figure represents the fitting of the experimental data to Equation 1. The resulting average value (three replicates) of thermal diffusivity from the data fitting was α = 0.0275 ± 0.003 cm^2/sec. Note that in the frequency range of 10–50 Hz of our experimental results, the samples are thermally thick. The same procedure was applied to the other samples. In Table I, we summarized the measured thermal diffusivities of the samples as a function of lime concentration.

RESULTS AND DISCUSSIONS

Crystallinity

The crystallinity evolution of cooked corn tortilla samples as a function of lime content are shown in Figures 3 and 4. Figure 3 illustrates the evolution of the X-ray diffractogram. Figure 4 illustrates the dependence of the sample crystallinity χ, as a function of the $Ca(OH)_2$ concentration. Two significant aspects in Figure 4 attract attention. First, the addition of small lime quantities up to a 0.2% concentration initially increases the sample crystallinity. On further increasing the lime content, the sample crystallinity decreases such that, at relatively high-lime contents the crystallinity is roughly equal to that of the original lime-free sample. Second, it looks as if the lime incorporation in our samples obeys two different kinetics. With lime content up to 0.2%, the crystallinity seems to obey first-order kinetics, approaching a saturation value of ≈0.2% concentration. For lime contents greater than this value, the sample crystallinity decreases with increasing lime content, following an S-shaped curve, which is typical of second-order kinetics. This suggests that we should interpret our data considering two regions of lime concentrations: a low-lime content region of growing crystallinity for concentrations <0.2%, and a high-lime content region for concentrations >0.2%, characterized by a loss of crystallinity.

First-order kinetics is mathematically described by a function which, starting from an initial value, approaches a saturation value without changing its curvature, as represented by curve (a) of Figure 5. It is represented by:

$$f = f_0 + \Delta f \, [1 - \exp(-x/\Delta x)] \qquad (2)$$

such that

$$f' = (f_s - f)/\Delta x \qquad (3)$$

Here, $f_s = f_0 + \Delta f$ is the saturation value; Δf is the excursion in approaching saturation; and Δx is the characteristic length of the control variable for completion of the process. In contrast, an S-shaped curve (probably best known example is the logistic curve) describes a second-order kinetics in which the system undergoes a transition between two saturation values taking place in a somewhat localized manner. That is, the transition occurs essentially at a given value x_c of the control variable during an excursion Δx with a marked change of its curvature as represented by curve (b) of Figure 5. The logistic curve may be written as:

$$f = f_0 + \Delta f \times [\zeta/(1 + \zeta)] \qquad (4a)$$

where

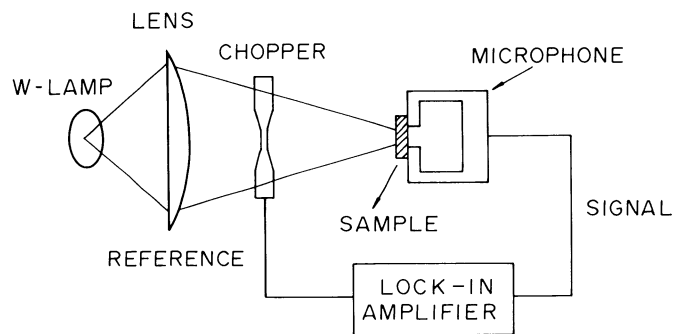$$\zeta = \exp [(x - x_c)/\Delta x] \qquad (4b)$$

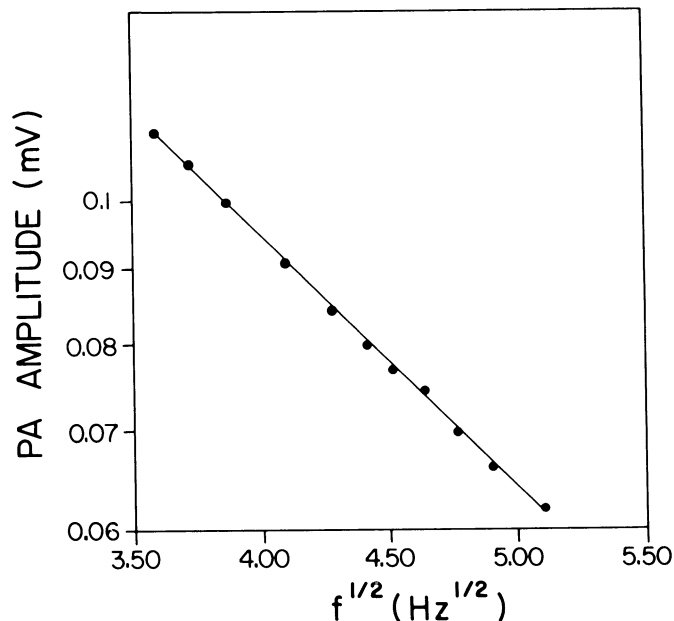Fig. 1. Experimental arrangement for thermal diffusivity measurements.

Fig. 2. Dependence of the photoacoustic (PA) signal amplitude as a function of the frequency (f) square root for the 300-μm thick tortilla without lime. Solid line represents the best fit of the experimental data to Eq. 1.
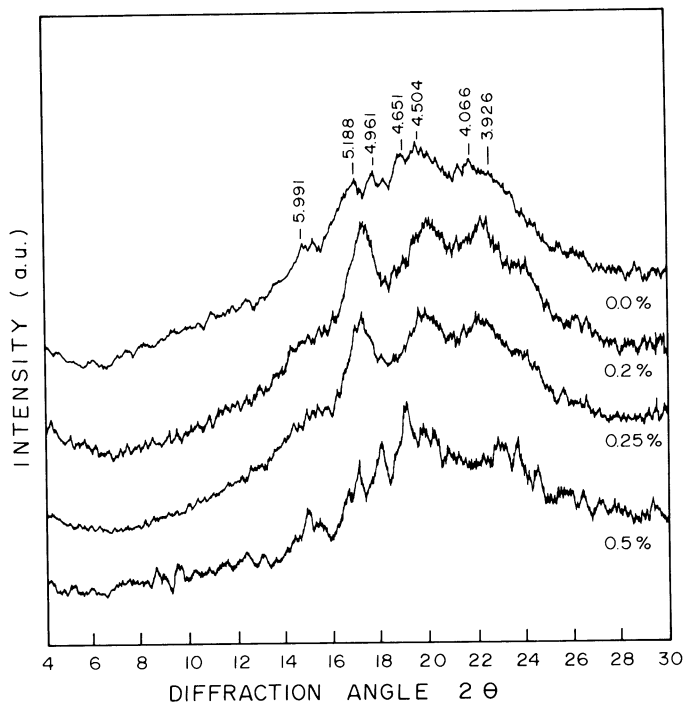

Fig. 3. X-ray diffractograms of cooked tortillas as a function of lime content (w/w). Numbers above peaks indicate interplanar d-spacings in Å.

In Equation 4, f_0 represents the initial saturation plateau; Δf is the overall excursion of f in going from the high to low saturation plateau; and x_c is the value of x at which f reaches halfway of its excursion, changing its curvature in a somewhat abrupt manner during a characteristic interval Δx around x_c. In terms of its fractional change, $\phi = (f_0 - f)/\Delta f$, the logistic curve obeys the differential equation:

$$\phi' = \phi \times (1 - \phi)/\Delta x \qquad (5)$$

Equation 5 indicates that the rate of change of ϕ is proportional to the fractional change times the excursion $(1 - \phi)$ left to reach the low saturation plateau. In the case of polymers, one example of first-order kinetics is given by the evolution of the thermal diffusivity of low-density polyethylene as a function of the immersion time in a crosslinking agent solution (dicumyl solution), reported by Cella et al (1989). An example of a logistic behavior was recently reported by Silva and Miranda (1994) for the dependence of the thermal diffusivity of iodine-doped cis-polyisoprene, as a function of the iodine doping concentration. The logistic behavior is typical of structural transitions.

The solid line in Figure 4 represents the results of the data fitting to first- and second-order kinetics, corresponding to the low-
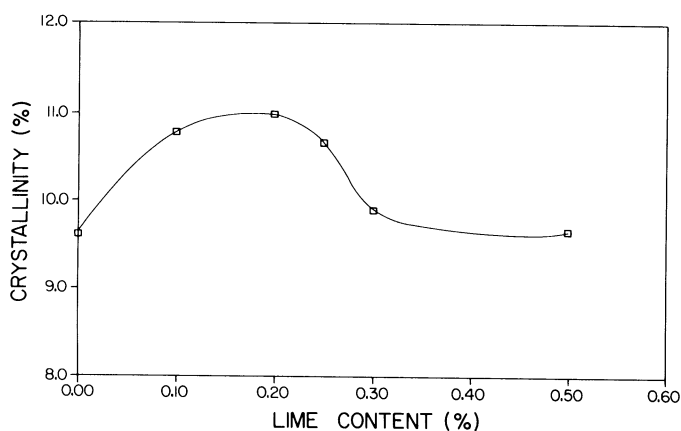
and high-lime content regions, respectively. In the low-lime content region, the crystallinity data fitting to Equation 2 yielded the following values for the fitting parameters: $f_0 = 9.62$, $\Delta f = 1.416$, $\Delta x = 0.0585$, with a deviation Chi-square parameter of 6.2×10^{-6}. In the high-lime content region, the crystallinity data fitting to Equation 4 gave the following values for the logistic curve parameters: $f_0 = 11.028$, $\Delta f = -1.368$, $x_c = 0.0196$, $\Delta x = 0.27$ with Chi-square $= 9.0 \times 10^{-8}$.
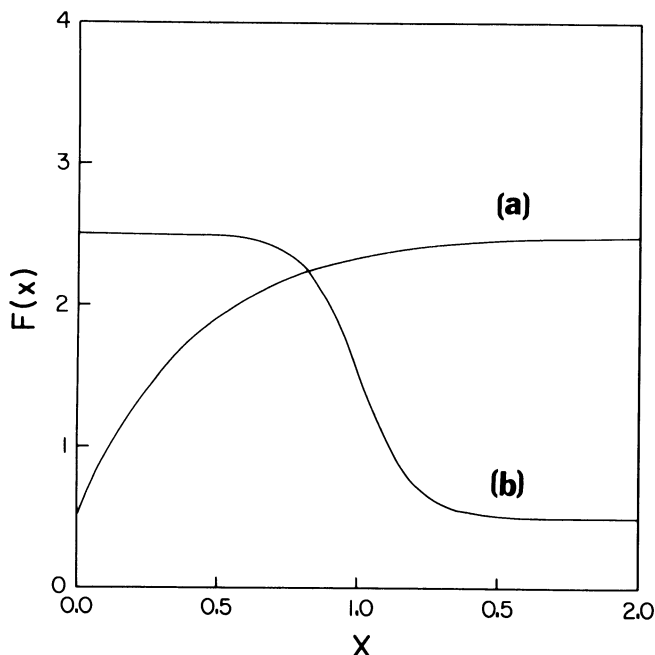
Some aspects of these results are worth noting. The observed enhancement of the sample crystallinity at a lime content up to 0.2% may be attributed to some calcium-induced crosslinking preventing the starch granules from swelling and collapsing, which results in a more rigid network. At the high-lime content region, the crystallinity tendency to recover the original value of the native lime-free sample seems to be associated with the calcium-amylose interaction (Gomez et al 1992).

Thermal Diffusivity

The thermal diffusivity ($\alpha = \kappa/\rho c$) measures essentially the thermalization time within the sample (the greater the thermal diffusivity, the lower the heating time). Here, κ denotes the thermal conductivity, ρ is the material density, and c is the heat capacity at constant pressure. The importance of α as a physical parameter to be monitored is due to the fact that, like the optical absorption coefficient, it is unique for each material. This can be appreciated from the tabulated values of α presented by Touloukian et al (1973) for a wide range of materials, such as, metals, minerals, foodstuffs, biological specimens, and polymers. Furthermore, the thermal diffusivity is extremely dependent upon the effects of compositional and microstructural variables (Vargas and Miranda 1988), as well as processing conditions, as in the case of polymers (Merté et al 1983, Torres-Filho et al 1988, Leite et al 1990).

In Figure 6, we present the results of the thermal diffusivity measurements of our tortilla samples as a function of the lime content. As in sample crystallinity, the thermal diffusivity plot exhibits two distinct behaviors as a function of the lime content. However, the kinetics of the thermal diffusivity evolution is quite distinct from that of the sample crystallinity χ. At low-lime contents (<0.2%), α increases slowly when compared to χ. In contrast, in the high-lime content region, α decreases faster than the crystallinity with increasing lime concentration. Furthermore, the sample crystallinity evolution was such that, after passing through a maximum at a lime content of $\approx0.2\%$, the final value of χ at the high-lime

Fig. 4. Crystallinity (%) of the tortilla samples as a function of lime content.

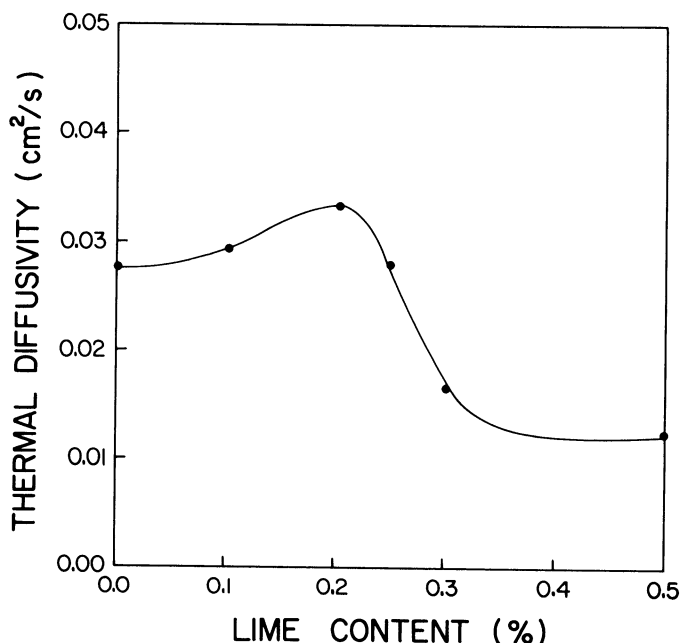Fig. 5. Typical first- (a) and second-order (b) kinetic functions.

Fig. 6. Thermal diffusivity of tortilla samples as a function of lime content.

region was roughly the same as that of the lime-free sample. The thermal diffusivity evolution, on the other hand, was such that, after growing to a maximum at ≈0.2%, it decreased to a lower value than that of the lime-free sample at the end of the high-lime content region. It is well known (Touloukian et al 1973) that the thermal diffusivity of more organized and symmetric materials is greater than those of amorphous and less organized materials. Thus, the overall behavior of α (Fig. 6) may be said to reflect the changes in the sample crystallinity. The increase of α is associated with the increased sample crystallinity, whereas its decreasing behavior at the high-lime contents is associated with the decrease of crystallinity. However, at the end of the high-lime content region, and contrary to the crystallinity behavior, the thermal diffusivity dropped to a value smaller than that of the lime-free sample. This indicates that some additional disorder is influencing the behavior of α. We attribute this to the fact that, in this region, some of the added lime remains as a distinct phase within the original network of dispersed starch granules. For this more disordered system we would expect α to be smaller than that for the lime-free sample.

The maximum in the thermal diffusivity indicates that a structural transition is occurring within the material. This result again reflects the changes in the sample crystallinity as a function of the lime incorporation. In Figure 7, we present a plot of both the thermal diffusivity and the sample's firmness as a function of the lime content. We note from this figure that, as the sample becomes more crystalline and rigid, the thermal diffusivity exhibits a
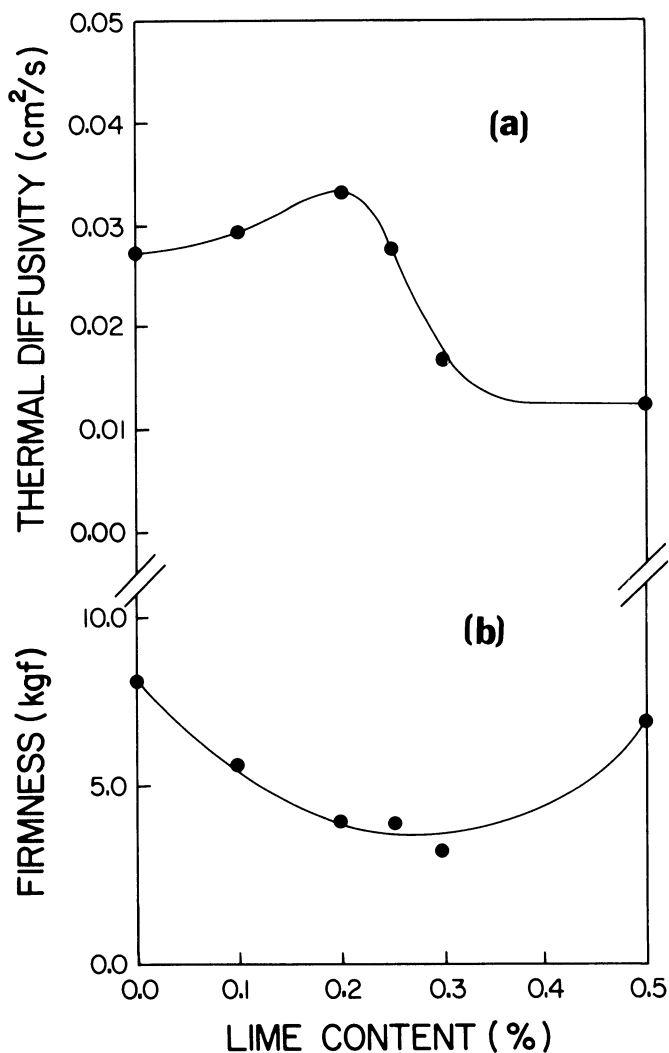
maximum at about the same position that the firmness goes through a minimum. This minimum in the sample's breaking force tells us that it became more rigid (less elastic) at this point.

The solid line in Figure 6 represents the data fitting to asymmetric Gaussian functions. That is, the asymmetric bell-shaped data of α were divided into two lime concentration regions and best fitted by two Gaussian functions having different widths and amplitudes but having the same peak position. Our result (in cm^2/sec) was:

$$0.027 + 0.006 \, e^{-[(x - 0.203)/0.098]^2} \text{ for } x < 0.203 \qquad (6a)$$
$$0.012 + 0.021 \, e^{-[(x - 0.203)/0.081]^2} \text{ for } x > 0.203 \qquad (6b)$$

The respective values of the fit deviation parameter Chi-square are 7×10^{-5} and 2.4×10^{-7}.

As to the sample firmness dependence upon the lime concentration, represented by the solid line in Figure 7, the data fitting was made using a simple parabolic curve. Denoting the firmness by Γ (in kgf), we have:

$$\Gamma = 8.133 - 33.166 \, x + 62.095 \, x^2 \qquad (7)$$

We note that Equation 7 predicts that the sample firmness is minimum at a lime content of 0.267 which is close to the value of 0.203 at which the maximum of the thermal diffusivity is positioned. It is worth noting that the overall dependence of Γ on the lime incorporation follows the general trend of reflecting the crystallinity changes. The firmness evolves from an original large value, goes through a minimum (indicating a more brittle regime), and then rises back to roughly the same original value, corresponding to a more elastic behavior.

To further support the suggestion that the behavior of the thermal diffusivity follows the corresponding changes of the sample crystallinity, we looked at the correlation between the thermal diffusivity and the sample crystallinity. The results are shown in Figure 8. The solid line in this figure represents the linear regression given by:

$$\alpha = 0.015 \, \chi - 0.132 \qquad (8)$$

This result strongly suggests that, indeed, the thermal diffusivity is simply manifesting the structural changes of our system due to the lime incorporation.
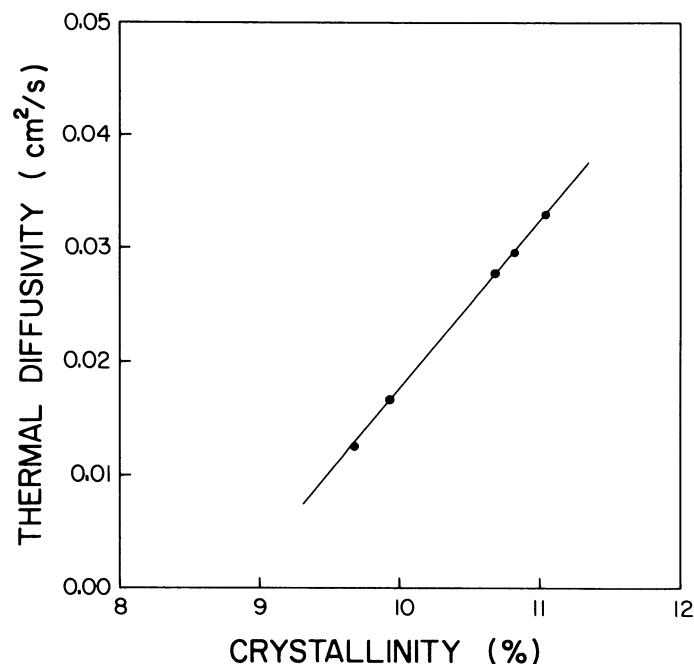
Fig. 7. Thermal diffusivity and breaking force of the tortilla samples as a function of lime content.

Fig. 8. Correlation between the thermal diffusivity (cm^2/sec) and the crystallinity (%) of the tortilla samples.

Dielectric Properties

In Figure 9, we plot the data listed in Table III for the dielectric constant (ε) and the electrical conductivity (σ) recorded at 10.2 kHz, as a function of the lime content. Both data exhibit a transition from a low to a high value as the lime content increases. This transition is accomplished with a Gaussian peak at $\approx 0.2\%$ lime content. A discontinuity in the dielectric constant, similarly to the thermal diffusivity, indicates that a structural transformation is taking place within the material. We also note that the dielectric constant peak value at $\approx 0.2\%$ lime content is quite close to that of water (≈ 80). This suggests that the calcium-induced starch crosslinking taking place at this lime concentration is followed by increasing water content. Furthermore, the final saturation values of both ε and σ at the high-lime content region are larger than those corresponding to their initial values at low-lime contents. This may be attributed to the fact that in this region we have an excess of unreacted lime forming a separate dispersed phase. The solid lines in Figure 9 represent the results of the data fitting to asymmetric Gaussian functions, similar to the calculations performed in the case of α. For the dielectric constant, the result is:

$$32.892 + 58.854\ e^{-[(x - 0.181)/0.0396]^2} \text{ for } x < 0.181 \quad (9a)$$
$$58.66 + 33.086\ e^{-[(x - 0.181)/0.021]^2} \text{ for } x > 0.181 \quad (9b)$$

for which the encountered values of the Chi-square fit parameter are 9.9 and 7.7, respectively.

For the ac dielectric conductivity $[\times 10^7\ (\Omega cm)^{-1}]$, the result is:

$$2.1195 + 4.7022\ e^{-[(x - 0.179)/0.046]^2} \text{ for } x < 0.179 \quad (10a)$$
$$4.4742 + 2.3475\ e^{-[(x - 0.179)/0.037]^2} \text{ for } x > 0.179 \quad (10b)$$

The respective values of Chi-square are 15×10^{-2} and 3.7×10^{-2}.

Infrared Absorption

In this section we present the results obtained for the IR absorption coefficients of the characteristic absorption bands of cooked tortilla samples. The absorption coefficients were obtained from the IR transmission spectra using Beer's law:
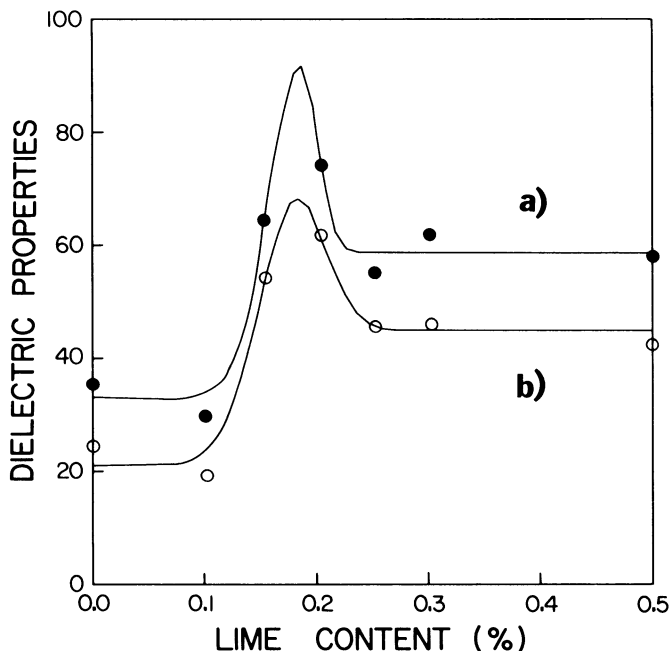
$$\beta = -(1/l)ln(T) \quad (11)$$

where T is the IR band transmittance, l is the sample thickness, and β is the corresponding absorption coefficient. The bands that best sensed the effects of the lime incorporation were at 3,350, 2,925, 1,161, 1,458, 710, and at 860 cm^{-1}. The band at 3,350 cm^{-1} corresponds to the stretching of bonded OH, whereas the bands at 2,925 and 1,161 cm^{-1} are assigned (Colthup et al 1975) to the stretching modes of CH and of CO bonds of C–OH and C–O–C groups, respectively. The band at 1,458 is attributed to CH$_2$ deformations and that at 710 cm^{-1} range corresponds to the C–H bond bending mode. The marked characteristics observed in the evolution of the IR absorption coefficients as a function of the lime incorporation may be summarized as follows. The absorption coefficients of all these bands reached a broad minimum between 0.1 and 0.3% lime concentration. The CO, CH, and the OH stretching modes at 1,161, 2,925, and 3,350 cm^{-1}, respectively, exhibited a relatively sharp growth of absorption coefficients at >0.3% concentration. In contrast, the absorption coefficients corresponding to the bending modes returned to their original values on increasing the lime content from 0.3 to 0.5%. These findings are clearly seen in Figures 10 and 11, in which we plot the absorption coefficients of the CO, CH, and OH stretching modes and the bending modes, respectively, as a function of the lime content. Up to 0.3% lime content, the evolution of the absorption coefficients as a function of the lime content was well described by a logistic curve. The results of fitting the corresponding data to a logistic curve was:

$$\beta = \beta_0 - \Delta\beta \times [\zeta/(1 + \zeta)] \quad (12)$$

where ζ is given by Equation 4b, are represented in these figures by the solid lines. In Table II, we summarize the values found for the fitting parameters β_0, $\Delta\beta$, x_c, and Δx.

The decrease of the absorption coefficients in the 0.1–0.3% lime concentration range means that the vibrations (or more precisely, the oscillator strength) are somehow getting rigid with smaller amplitude. In other words, the dipole moments corresponding to these vibrational modes become smaller with lime incorporation. Once again, this is consistent with the increase of the sample crystallinity of this concentration range. On further increasing the lime concentration to >0.3%, the bending modes recover their original strength. The CO, CH, and OH stretching
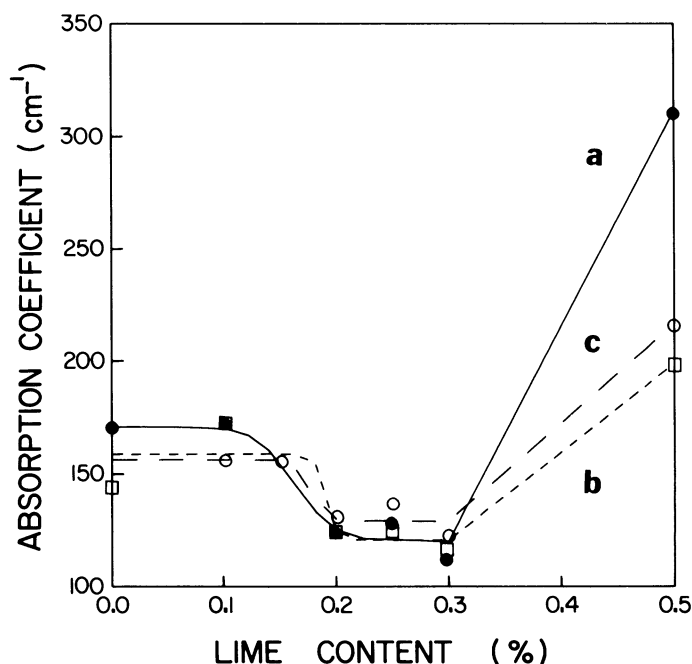

Fig. 9. Dielectric constant (a) and ac electrical conductivity (b), in $(\Omega cm)^{-1}$ $\times 10^6$ of the tortilla samples, recorded at 10.2 kHz as a function of lime content.

Fig. 10. Absorption coefficients corresponding to bands of the tortilla samples as a function of the lime content. **a,** 1,161; **b,** 2,925; **c,** 3,350 cm^{-1}.

modes, on the other hand, exhibit a sharp increase for lime addition to >0.3% concentration. From its definition, the absorption coefficient is written as the product of the concentration times the extinction coefficient:

$$\beta = x\,k \qquad (13)$$

where x denotes the concentration of absorbing centers and k is the optical extinction coefficient. The fact that, on increasing x, β is decreasing, means that the extinction coefficients should be decreasing. This, as mentioned above, is attributed to the more rigid character that develops upon the lime incorporation. It was manifested in all investigated properties. Furthermore, this decrease of β follows essentially a logistic behavior. This entails that this process is accompanied by a threshold. In fact, looking at Table II, we note that the logistic decrease of β values occurs at a critical value of the lime content (x_c) of $\approx 0.17\%$, on the average. At $\approx 0.3\%$ lime content, the behavior of the absorption coefficients is quite distinct. Stretching modes increase their absorption coefficients on increasing the lime content, whereas the bending modes absorption coefficients remain practically constant at their corresponding original lime-free values. This suggests that the way the calcium ions are interacting with the starch is markedly different in these two concentration regions. In one case, the Ca ions are interacting with our matrix promoting an enhancement of the starch crosslinking. This reaction takes place in a critical concentration range, as manifested by the logistic behavior of β and χ, as well as by the sharpness of the dielectric and thermal diffusivity changes. At $\approx 0.3\%$ lime concentration, the Ca ions seem to be interacting with the original undeformed matrix. This conclusion is based on two facts: 1) the ring modes seem to remain unaffected by the lime addition; 2) the increase of the stretching modes absorption coefficients (Fig. 9) also suggests that their extinction coefficients are constant. If the extinction coefficients increased (larger dipole moments), it would imply that the system gets more elastic (amorphous). Thus, we are tempted to say that at >0.3% concentration, the Ca ions are more likely to be interacting on the surface of the starch granules. If they were interacting within the bulk, we would observe a decrease in the system's crystallinity due to the enhancement of the starch gelatinization and granule degradation.
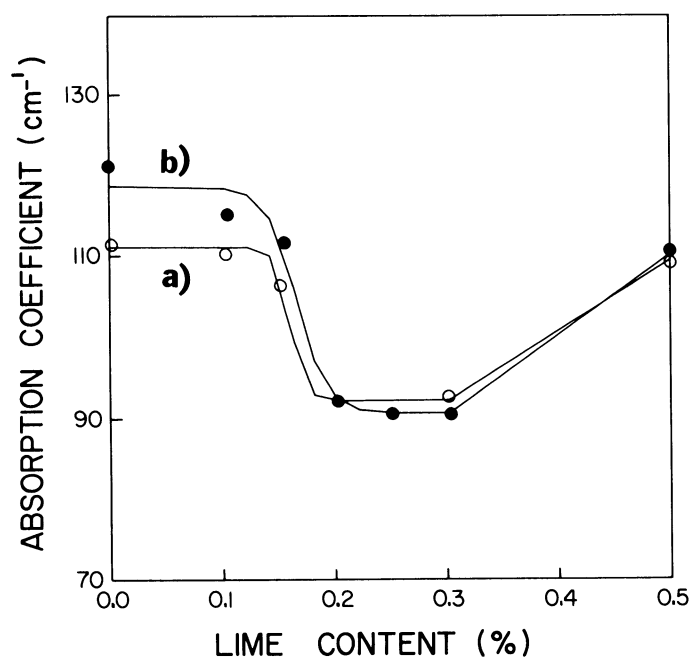
We would like to further stress that the thermal diffusivity and firmness data all suggest that at a critical lime concentration of $\approx 0.2\%$, a calcium-induced crosslinking takes place. This reaction seems to be quite localized. The dielectric measurements confirm this hypotesis of concentration-dependent calcium-induced crosslinking. Both ε and σ exhibited pronounced peaks at this critical lime concentration. Moreover, the dielectric constant data at $\approx 0.2\%$ lime content raised to a value quite close to that of water, indicating that this crosslinking is accompanied by water retention. One possible explanation for the observed lime-induced crosslinking changes of the measured physical properties may be viewed as follows. As is well known (Kerr 1950, Whistler and Paschall 1965, Banks and Greenwood 1975), the availability of hydroxyl groups in starch is the main reason for the association of starch molecules through H bonds. In a normal state, the neighboring OH groups of starch molecules are linked through one or more H_2O molecules, forming a chain with many side branches as an entangled mass (Fig. 12a). Alkalis, as well as salts of the lyotropic series (NaI, NaBr, etc.), among other salts, are also known (Whistler and Paschall 1965) to be effective starch-swelling agents. These agents seem to act essentially to destroy the association (through H bonds) of water molecules, that is to reduce the aggregates of water molecules to smaller units approaching the dimensions of single molecules. This would, in turn, increase the penetrating power of water and, consequently, its availability to the crosslinking of starch molecules. Furthermore, it is also quite possible (Whistler and Paschall 1965) that the agents that weaken the H bonds between the water molecules also tend to weaken the H bonds through which the starch molecules are linked. This suggests that, in the present case of lime incorporation, the strong Ca-amylose interaction may also contribute, as another auxiliary route, to the starch crosslinking, through the formation of a calcium bridge (Fig. 12b). In addition to these points, it is known that by controlling the concentration of swelling agents, it is possible to vary the swelling speed. At low-swelling agent concentrations, water is slowly and reversibly taken up and limited swelling occurs.

Putting all these facts together, one is led to the conclusion that at low-lime contents (up to 0.2% concentration), the observed crystallinity enhancement may be attributed to the swelling action of lime due to the moderate amount of water taken up, and

Fig. 11. Absorption coefficients of the bands of the tortilla samples as a function of the lime content. a, 1,458; b, 710 cm^{-1}.
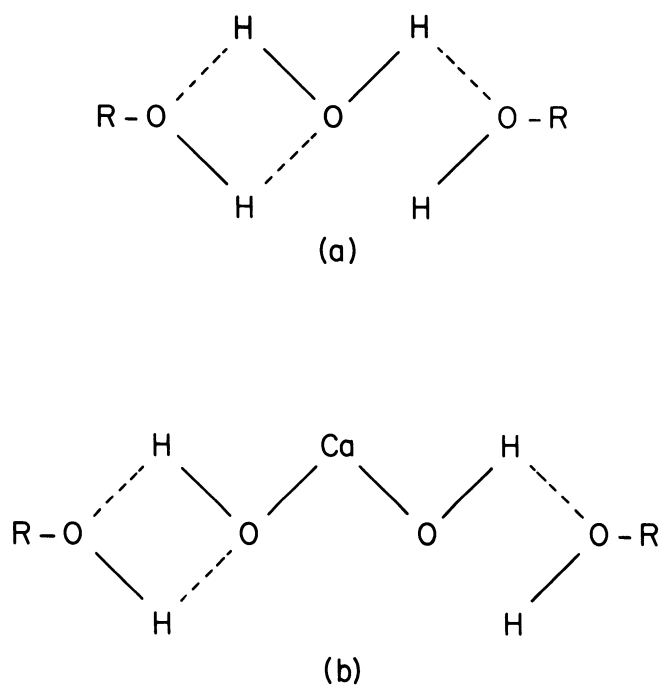

Fig. 12. Association of starch through water (a) and calcium hydroxide (b) molecules. H bonds are represented by dots.

probably also helped by the direct intervention of calcium as suggested in Figure 11b. At high-lime contents, the evolution of the IR absorption coefficients, together with the recovery of the original sample crystallinity, points to an anchorage of the Ca ions on the surface of the starch granules. In this way, the strong Ca-amylose interaction would prevent the water being taken up, avoiding swelling and degradation of the starch granules.

CONCLUSIONS

In this article, we have investigated the evolution of the thermal, dielectric, and IR spectroscopic properties of corn-alkaline cooked tortillas as a function of their lime contents. The changes of these physical properties were further supplemented by additional measurements of the sample crystallinity and breaking force. It was shown that the additional information provided by the structure-sensitive properties, such as the dielectric constant, thermal diffusivity, and the breaking force can indeed be an important complementary support to the chemically sensitive IR spectroscopic data.

From the food processing point of view, these results have two main implications, regarding both the cooking time and the texture of the final product. The thermal diffusivity essentially measures the sample's thermalization time, such that the smaller its value, the longer it takes for the sample's temperature to stabilize. This suggests that for faster cooking products, the optimum lime content should be $\approx 0.2\%$. In fact, looking at Table I, we see that at this lime content (where α is largest), the cooking time is $\approx 11\%$ smaller than that of the lime-free sample. As to the tortilla's texture, the lime content of 0.2% corresponds to the point at which the sample would be more crystalline and, therefore, more crispy. Thus, if one wants a product that is crispy and cooks fast, one should work with the optimum lime content of 0.2%. In particular, the usefulness of the PA technique for obtaining the thermal properties of tortillas has been shown to be an important tool in engineering analysis and can serve as a product quality evaluation method associated with the general processing and storage of starchy foods.

LITERATURE CITED

ALEXANDER, K. and KING, C. J. 1985. Factors governing surface morphology of spray-dried amorphous substances. Drying Technol. 3:321.

ALVARADO-GIL, J. J., ZELAYA-ANGEL, O., SANCHEZ-SINENCIO, F., YAÑEZ-LIMÓN, M., VARGAS, H., FIGUEROA, J. D. C., MARTINEZ-BUSTOS, F., MARTINEZ, J. L., GONZALEZ-HERNANDEZ, J. 1995. Photoacoustic monitoring of processing conditions in cooked tortillas: Measurement of thermal diffusivity. J. Food Sci. 60:438.

BANKS, W., and GREENWOOD, C. T. 1975. Starch and Its Components. J. Wiley: New York.

CELLA, N., VARGAS, H., GALEMBECH, E., GALEMBECK, F., and MIRANDA, L. C. M. 1989. Photoacoustic monitoring of crosslinking reactions in low-density polyethylene. J. Polym. Sci. 27:313.

COLTHUP, N. B., DALY, L. H., and WIBERLE, S. E. 1975. Introduction to Infrared and Raman Spectroscopy. Academic Press: New York.

DONOVAN, J. W. 1979. Phase transitions of starch-water system. Biopolymers 18:263.

GOMEZ, M. H., LEE, J. K., McDONOUGH, C. M., WANISKA, R. D., and ROONEY, L. W. 1992. Corn starch changes during tortilla and tortilla chip processing. Cereal Chem. 69:275.

HERRINGTON, T. M., and BRANDFIELD, A. C. 1984. Physico-chemical studies of sugar glasses. I. Rates of crystallization. J. Food Technol. 19:409.

HOLLINGER, G., KUNIAK, L., and MARCHESSAULT, R. H. 1974. Thermodynamic aspects of gelatinization and swelling of crosslinked starch. Biopolymers 13:879.

KERR, R.W. 1950. Chemistry and Industry of Starch. Academic Press: New York.

LACHAINE, A., and POULET, P. 1984. Photoacoustic measurement of thermal properties of a thin polyester film. Appl. Phys. Lett. 45:953.

LEITE, N. F., FRANZAN, A. H., TORRES-FILHO, A., and MIRANDA, L. C. M. 1990. Dielectric constant, optical transmission and thermal diffusivity monitoring of iodine-impregnated polystyrene films. J. Appl. Polym. Sci. 39:1361.

LEVINE, H., and SLADE, L. 1988. Principles of cryostabilization technology from structure/property relationships of carbohydrate/water systems. A review. Cryo-Letters 9:21.

MANSANARES, A. M., BENTO, A. C., VARGAS, H., LEITE, N. F., and MIRANDA, L. C. M. 1990. Photoacoustic measurement of the thermal properties of two-layer systems. Phys. Rev. B42:4477.

MARQUEZINI, M. V., CELLA, N., VARGAS, H., and MIRANDA, L. C. M. 1991. Open photoacoustic cell spectroscopy. Meas. Sci. Technol. 2:396.

MERTÉ, B., KORPIUM, P., LUSCHER, E., and TILGNER, R. 1983. Thermal diffusivity of polymer foils–semicrystalline PET and PE–as a function of drawing. J. Phys. (Paris) Colloq. 44:463.

PAREDES-LOPEZ, O., and SAHAROUPULOS, M. E. 1982. Scanning electron microscopy studies of limed corn kernels for tortilla making. J. Food Technol. 17:691.

PERONDI, L. F., and MIRANDA, L. C. M. 1987. Minimal-volume photoacoustic cell measurements of the thermal diffusivity: Effect of thermoelastic sample bending. J. Appl. Phys. 62:2955.

ROBLES, R. R., MURRAY, E. D., and PAREDES-LOPEZ, O. 1986. Physico-chemical changes of maize starch during the lime-cooking treatment for tortilla making. Int. J. Food Sci. Technol. 23:91.

ROOS, Y. H. 1987. Effect of moisture on the thermal behavior of strawberries using differential scanning calorimetry. J. Food Sci. 52:146.

ROOS, Y. H., and KAREL, M. 1991. Plasticizing effect of water on thermal behavior and crystallization of amorphous food models. J. Food Sci. 56:38.

SALTMARCH, M., and LABUZA, T. P. 1980. Influence of relative humidity on the physico-chemical state of lactose in spray-dried sweet whey powders. J. Food Sci. 45:1231.

SILVA, M. D., and MIRANDA, L. C. M. 1994. Modifications of the dielectric and thermal properties of vulcanized natural rubber due to iodine doping. Phys. Rev. B49:12646.

SIMATOS, D., and KAREL, M. 1988. Characterization of the condition of water in foods–physico-chemical aspects. In: Food Preservation by Water Activity Control. C. C. Seow, ed. Elsevier: Amsterdam.

SLADE, L., LEVINE, H., and FINLAY, J. W. 1989. Protein-water interactions: Water as a plasticizer of gluten and other protein polymers. In: Protein Quality and the Effects of Processing. R. D. Phillips and J. W. Finlay, eds. Marcel Dekker: New York.

TORRES-FILHO, A., PERONDI, L. F., and MIRANDA, L. C. M. 1988. Photoacoustic monitoring of epoxy-based adhesive curing. J. Appl. Polym. Sci. 35:103.

TORRES-FILHO, A., LEITE, N. F., CELLA, N., VARGAS, H., and MIRANDA, L. C. M. 1989. Photoacoustic investigation of iodine-doped polysterene. J. Appl. Phys. 66:97.

TOULOUKIAN, Y. S., POWEL, R. W., HO, Y. C., and NOCOLASU, M. C. 1973. Thermal Diffusivity. Plenum Press: New York.

TREJO-GONZALEZ, A., MORALES, A., and WILD-ALTAMIRANO, C. 1982. The role of lime in the alkaline treatment of corn tortilla preparation. Page 145 in: Modification of Proteins: Food, Nutritional and Pharmacological Aspects. Advances in Chemistry Series 198. R. E. Feeney and J. R. Whitaker, eds. Am. Chem. Soc.: Washington, DC.

VARGAS, H., and MIRANDA, L. C. M. 1988. Photoacoustic and related photothermal techniques. Phys. Rep. 161:43.

WHISTLER, R., and PASCHALL, E. F. 1965 Eds. Starch Chemistry and Technology. Vol. 1. Academic Press: New York.